Industrial Chemistry & Materials

ROYAL SOCIETY OF CHEMISTRY

PAPER

View Article Online
View Journal | View Issue

Cite this: *Ind. Chem. Mater.*, 2026, **4**, 237

Carbon-supported Ni nanoparticles in CO_2 methanation: role of a superficial NiO shell observed by *in situ* TEM†

Katherine E. MacArthur,‡*[a] Liliana P. L. Gonçalves,‡[bcd] Juliana P. S. Sousa,[b] O. Salomé G. P. Soares,[cd] Hans Kungl,[e] Eva Jodat,[e] André Karl,[e] Marc Heggen,[a] Rafal E. Dunin-Borkowski,[a] Shibabrata Basak,*[e] Rüdiger-A. Eichel,[efg] Yury V. Kolen'ko[b] and M. Fernando R. Pereira*[cd]

CO_2 methanation offers a pathway to produce a carbon-neutral methane fuel. Although a number of research efforts have been conducted on this topic, a greater understanding of the mechanism of the reaction, which is still under debate, is needed. Here, using *in situ* transmission electron microscopy, we provide direct insights into the dynamics of a metallic nickel catalyst supported on activated carbon during CO_2 methanation. The keys to the high performance of the catalyst are the *in situ* formation and dynamic behavior of a Ni@NiO core@shell nanostructure. Based on the detailed electron microscopy investigation, the mechanism of such nanostructure formation during methanation is proposed. Our studies revealed that the deactivation of the catalyst is not due to the accumulation of carbon coke over nickel nanoparticles, but an increase in the size of the nickel nanoparticles that is responsible for the deactivation of the catalyst over time.

Keywords: CO_2 valorization; Hydrogenation; *in situ* TEM; Carbon catalysts; Core–shell nanoparticles; Microstructure.

Received 1st March 2025,
Accepted 15th July 2025

DOI: 10.1039/d5im00033e

rsc.li/icm

1 Introduction

The CO_2 methanation reaction has been the subject of intense studies, since it offers an interesting pathway to produce a carbon-neutral methane fuel (e-CH_4), thus combating the CO_2 emissions to the atmosphere.[1–5] Mostly Ni-based catalysts supported on a variety of supporting materials, such as metal oxides,[6–8] zeolites,[9] metal organic frameworks,[10] and carbons,[3,11–18] are used for CO_2 methanation. Interestingly, the supporting material plays a major role in the catalyst's performance, and it has been demonstrated that the same active phase, such as Ni nanoparticles, can present different activity, selectivity, and stability, depending upon the supporting material being used.[3,5,11,19] Besides the fact that CO_2 methanation involves reactant diffusion, adsorption, surface reaction, product desorption, and diffusion, the metal–support interactions can also play a role in the catalytic mode of action, which is consequently reflected in the performance of the catalyst.[3,20]

Notably, the mechanism of CO_2 methanation is still under debate. The proposed mechanisms are largely governed by the catalytic system and the reaction conditions, and the methanation could proceed through (i) the associative pathway, in which CO_2 is adsorbed associatively with a former adsorbed H atom, forming formate as an intermediate, and (ii) the dissociative pathway, where CO_2 is dissociated in CO, which is the main intermediate of the reaction.[4] The mechanism behind nickel-catalyzed CO_2 methanation involves the dissociation of H_2 over the Ni nanoparticles, while CO_2 adsorption usually occurs on the supporting material or nickel–support interface with dissociation and

[a] *Ernst Ruska-Centre for Microscopy and Spectroscopy with Electrons, Forschungszentrum Jülich, 52425 Jülich, Germany. E-mail: k.macarthur@fz-juelich.de*
[b] *International Iberian Nanotechnology Laboratory (INL), Braga 4715-330, Portugal*
[c] *LSRE-LCM – Laboratory of Separation and Reaction Engineering – Laboratory of Catalysis and Materials, Faculty of Engineering, University of Porto, Rua Dr. Roberto Frias, 4200-465 Porto, Portugal. E-mail: fpereira@fe.up.pt*
[d] *ALiCE – Associate Laboratory in Chemical Engineering, Faculty of Engineering, University of Porto, Rua Dr. Roberto Frias, 4200-465 Porto, Portugal*
[e] *Institute of Energy Technologies – Fundamental Electrochemistry (IET-1), Forschungszentrum Jülich GmbH, Jülich, Germany. E-mail: s.basak@f-juelich.de*
[f] *Institute of Physical Chemistry, RWTH Aachen University, Aachen, Germany*
[g] *Faculty of Mechanical Engineering, RWTH Aachen University, Aachen, Germany*
† Electronic supplementary information (ESI) available: Detailed experimental procedures, together with the additional TEM data and a video. See DOI: **https://doi.org/10.1039/d5im00033e**
‡ These authors contributed equally.

subsequent adsorption of the resultant carbonyl on Ni nanoparticles.[21]

A comprehensive understanding of the behavior of the supported Ni catalyst under reaction conditions, coupled with a thorough elucidation of the associated reaction mechanism, is imperative for facilitating the rational design of high-performance catalyst materials. Hence, *in situ* techniques are particularly important and have been extensively used to elucidate the mechanism of CO_2 methanation over various supported catalytic systems. For instance, *in situ* infrared (IR) spectroscopy has been used for underpinning the reaction intermediates,[20,22–25] while X-ray photoelectron spectroscopy (XPS) and near edge X-ray absorption fine structure (NEXAFS) have been employed to elucidate the chemical nature of the real catalysts under methanation conditions.[26,27] At the same time, the fine microstructural modifications, that the supported Ni catalysts undergo during CO_2 methanation, have been studied to a less extent. For example, deactivation of the Ni catalysts is often attributed to the sintering of the Ni nanoparticles and/or coke building up on the active phase, which has been investigated by *ex situ* transmission electron microscopy (TEM).[4,28] Importantly, *in situ* observation of fine microstructural modifications should assist in understanding and further developing active, selective and stable methanation catalysts. Hence, in this study, *in situ* TEM is applied to elucidate the behavior of the Ni catalyst supported on the reduced activated carbon during CO_2 methanation, affording insight into the presently lacking understanding of the catalyst's real microstructure and its dynamics.

The understanding and atomic level information provided by aberration-corrected TEM is unparalleled, particularly for the study of catalyst nanoparticles. The development of a specialized microelectromechanical system (MEMS)-based sample holder allows us to contain gas near the sample at more than 1 bar pressure with precise control over temperature, as well as gas flow and gas compositions.

In this study, we have utilized a MEMS-based nanoreactor in which two Si/SiNx chips are positioned on top of each other and sealed with an O-ring, allowing for a maximum gas pressure of up to 2 bar. A 5 μm spacer on the bottom chip guides the gas mixture from the gas supply system towards the microheater. The system can be heated up to 1000 °C with small power consumption (in the range of mW), thus offering a low drift, while the 30 nm thin electron transparent SiN_x windows, that are present in these chips, allow transmission of electron beams, thus affording structural characterization of the samples under realistic reaction conditions.

2 Results and discussion

Our earlier study[3] demonstrated excellent CO_2 methanation performance of a Ni catalyst supported on reduced activated carbon (Ni/ACR). Interestingly, after 90 h of CO_2 methanation at 450 °C and 0.1 MPa, with 10% H_2, 40% CO_2 and 50% He, a distinct crystalline shell of Ni oxide was formed on the surface of the Ni nanoparticles supported on ACR observed *via ex situ* TEM. Fig. 1 shows TEM images of the Ni nanoparticles pre- and post-reaction, with the oxide shell of thickness 2–3 nm highlighted in Fig. 1b. The observation of a Ni oxide shell on the Ni nanoparticles after prolonged CO_2 methanation was intriguing, as it contradicted the prevailing expectation that metallic Ni was the active phase of the reaction. However, these samples were transferred in air, after cooling to room temperature, for the post-reaction analysis; therefore, it was unclear whether the oxide shell was formed during the air transfer or as a consequence of the reaction conditions. Understanding this detail, along with the possible deactivation mechanism of the supported Ni catalyst, will not only shed light on the debatable methanation mechanism but also pave the pathway for engineering improved catalysts.

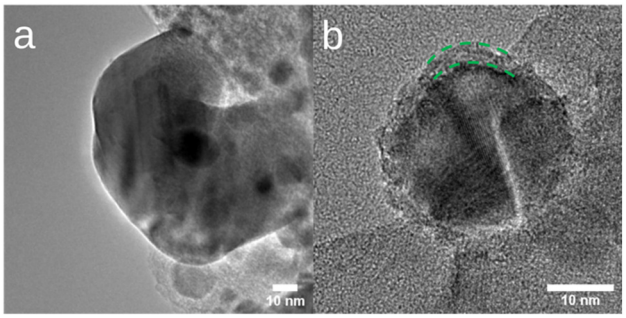

Fig. 1 The *ex situ* TEM analysis results of the Ni/ACR catalyst before (a) and after (b) CO_2 methanation for 90 h. The resultant Ni@NiO core@shell nanostructure is highlighted by the green dashed lines in (b).

To exactly replicate the reaction conditions, the drop-cast Ni/ACR catalyst was first reduced under a H_2 environment (4% H_2 with N_2 as the carrier gas at 1 bar pressure) at 400 °C, and then imaged under the reactive H_2 and CO_2 gases providing methanation conditions. It is found that once a temperature of 450 °C is reached under the reactive gases, the Ni nanoparticles began to dynamically change shape whilst still retaining crystallinity. Fig. 2(a–d) shows the dynamics of such a nanoparticle within the thick ACR supporting material. The arrows highlight the dynamic reduction-growth of the nanoparticle that simulates a 'breathing' behaviour. We believe that this 'breathing' behavior is the macroscopic manifestation of a dynamic equilibrium at the nanoscale. It likely involves the continuous, competitive oxidation of the nickel surface by CO_2 to form NiO, and the simultaneous reduction of this oxide shell by H_2. The observed shape changes reflect the local fluctuations in the rates of these opposing reactions. The corresponding breathing process can be better portrayed in Movie S1 in the ESI.† It should be pointed out that the reduction performed at 400 °C during the *in situ* experiments followed from our previous work on the same Ni on the ACR sample, where during the temperature programmed reduction (TPR) experiment, it

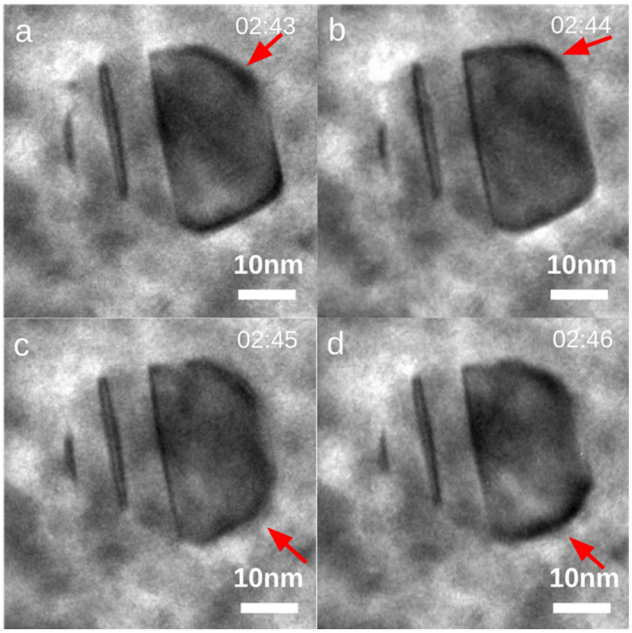

Fig. 2 *In situ* time-series of TEM images showing a dynamic active particle away from the edge of the carbon support, from time 2:43 to 2:46 (a–d). The area that has undergone dynamic changes is indicated by the red arrows.

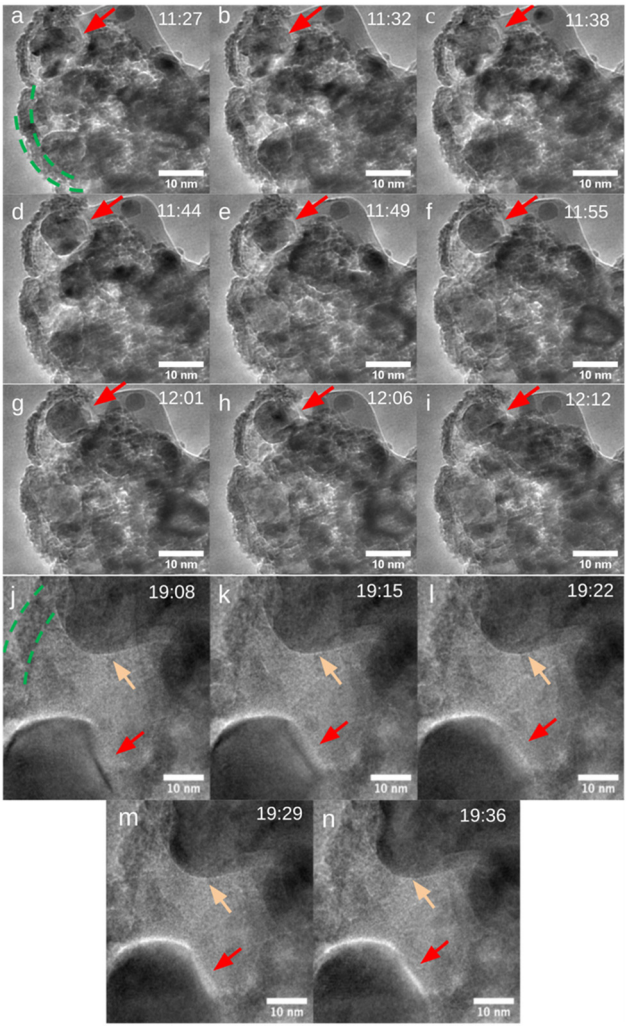

Fig. 3 Low-magnification *in situ* time-series of TEM images for active nanoparticles changing dynamically under reaction conditions without H_2 pre-treatment (a–i); *in situ* time-series of TEM images under reaction conditions with H_2 pre-treatment showing a non-active particle (pointed by orange arrows) in the top right and an active particle (pointed by red arrows) in the bottom left (j–n). The oxide shell is visible in both cases – marked in green. The timestamp in the top right-hand corner of each image shows the time in minutes and seconds since the methanation reaction conditions were reached. One example of the dynamic behaviour of the nanoparticles is pointed by the red arrows.

was verified that even the Ni species that interact more strongly with the carbon were reduced at *ca.* 380 °C.[3]

To determine whether the dynamic behavior is impacted by the H_2 pre-treatment, Fig. 3 compares *in situ* results where the sample was initially reduced in an H_2 atmosphere to another set of experiments where the H_2 pre-treatment was not used. Overall, like the nanoparticle shown in Fig. 2, Fig. 3 shows the dynamic behaviour of Ni nanoparticles towards the edge of the ACR supporting material under the dynamic conditions. The red arrows highlight a few of these changes in two particles, as examples. Interestingly, the presence of an oxide shell is clearly visible in both cases. The green dashed lines in Fig. 3a and j highlight the oxide shell. The high-resolution image in Fig. S1† shows the polycrystalline nature of the oxide layer outside the nanoparticles. The apparent absence of such an oxide layer for the particle shown in Fig. 2 is most likely due to the difficulty to resolve such a layer in the presence of the thick ACR supporting material. Notably, it is clear that the particles towards the edge of the ACR support changed more dynamically and, in some cases, appear almost molten, rolling around within an oxide shell. This is likely due to improved mass transport, allowing for more efficient diffusion of the CO_2 and H_2 reactant gases to the nanoparticle surface compared to particles embedded deeper within the porous support. The red arrows in Fig. 3a–i indicate one such nanoparticle. This behaviour was seen regardless of whether or not the reducing H_2 pre-treatment was applied, as observed in Fig. 3a–i (the sample without H_2 reduction) *vs.* Fig. 3j–n (similar sample, under similar conditions, but with H_2 reduction pre-treatment). Primarily, we noticed that the formation of the oxide shell was not a mechanism of the deactivation of the particles. In fact, the most dynamic behaviour was seen for particles exhibiting an oxide shell, thereby suggesting a permeable structure in which the reactive gases can penetrate to reach metallic Ni active sites. Thus, we demonstrated that the observed NiO shell after CO_2 methanation for 90 h (Fig. 1) is not a result of the non-reduced catalyst but rather formed under reaction conditions, as observed during the *in situ* TEM studies.

Using *in situ* XPS, Heine and co-workers[29] reported the formation of NiO even at room temperature in CO_2 gas alone, which requires the transfer of two electrons from

metallic Ni to the CO_2 molecule, forming Ni^{2+} due to the oxidation of Ni^0 and CO due to the reduction of CO_2. However, after the introduction of H_2 into the system mimicking methanation conditions, NiO species were found to be reduced again to metallic Ni^0. In another interesting study that uses *in situ* XPS and *in situ* NEXAFS spectroscopies, Giorgianni and co-workers[26] reported a similar behavior, wherein the metallic Ni surface was found to oxidize rapidly upon exposure to CO_2. Under methanation conditions (*i.e.*, CO_2 + H_2), while *in situ* XPS revealed that Ni is predominantly in a reduced state, *in situ* NEXAFS indicated that the shell of Ni nanoparticles is prevalently in a Ni^{2+} state due to incomplete reduction. Interestingly, Mutz and co-workers[30] showed that, in the presence of CO_2, Ni starts to oxidize after the removal of H_2 from the gas flow. When H_2 is again introduced into the stream, the reduced fraction of metallic Ni was found to increase to 94%, yet having a 6% fraction of oxidized Ni. In our study, we would not expect the Ni nanoparticles to oxidize, since they are under an atmosphere rich in H_2; however, CO_2 should be responsible for the oxidation of the surface of the Ni nanoparticles, thus forming the NiO shell according to the following reaction: Ni + CO_2 = NiO + CO. The Ni^0 species can be oxidized by CO_2 to form Ni^{2+} species, activating the CO_2 as well, to form CO.[31] Importantly, an experiment where only CO_2 gas was used (Fig. S2†) shows that the presence of both H_2 and CO_2 is required for the oxide-shell formation (*i.e.*, only surface oxidation), since in the presence of CO_2 alone, no oxide shell can be seen. Therefore, the synergetic relationship between CO_2 and H_2 should be responsible for the formation of the Ni@NiO core–shell structure during CO_2 methanation, as observed herein.

The formation of this Ni@NiO core@shell structure under reaction conditions might be one of the reasons for the good performance of this catalyst. On the one hand, the NiO formation in close contact with the supporting carbon material, where CO_2 is adsorbed, leads to the activation of this molecule,[25,31] while the Ni^0 in the core is responsible for H_2 dissociation, since the dynamic nature of the oxide shell allows for the diffusion of the H_2 to the metallic Ni^0 core of the nanoparticles. This way, both reactants can be in close contact, which facilitates the reaction. On the other hand, NiO might present oxygen vacancies, which are known to induce the dissociation and activation of CO_2 on the surface of the catalyst.[32] It has been reported before that the rate-determining step for the CO_2 methanation reaction should be related to the availability of adjacent adsorbed H to hydrogenate adsorbed CO;[33] thus, this proximity of CO_2 activation and CO formation on the NiO shell and H_2 dissociation in the Ni core might explain the good performance on the catalyst.[3]

After examining the dynamic behaviour of the particles under a reactive methanation environment, we then explored the mechanisms of deactivation of the catalyst. The main deactivation mechanism was observed to be related to a particle size increase. This can be observed in Movie S2,† obtained at 450 °C in the presence of both H_2 and CO_2. The larger particles demonstrated no dynamic changes, while the smaller particles demonstrated to be very active. Upon cooling, the particle structures stabilised to fill the oxide shell again (this can be seen in Fig. S3†), yielding a structure that matches the original *ex situ* characterisation (Fig. 1b). Finally, post *in situ* energy dispersive X-ray spectroscopy analysis in scanning TEM mode (STEM-EDX) was performed to confirm the presence of a 2–3 nm thick NiO shell (Fig. 4(a–f)). The heating and gas profile during these *in situ* experiments can be found in Fig. S4.†

Particle size distribution was not thoroughly studied in this work; however, since methanation is a known structure-sensitive reaction, the catalyst particle size is an important aspect. Thus, further experiments should be carried out to address this topic.

Our experimental *in situ* TEM findings have demonstrated that the nickel oxide shell observed on the catalytic Ni nanoparticles supported on reduced activated carbon in our previous study[3] is in fact formed under reaction conditions

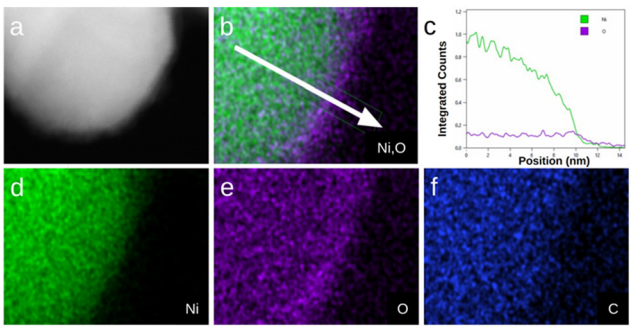

Fig. 4 Post *in situ* STEM–EDS analysis of the catalyst nanoparticle showing the annular dark-field STEM (a), Ni, O EDS overlay map (b), variation of Ni and O count along the arrow direction (c), and corresponding Ni (d), O (e), and C (f) EDS map.

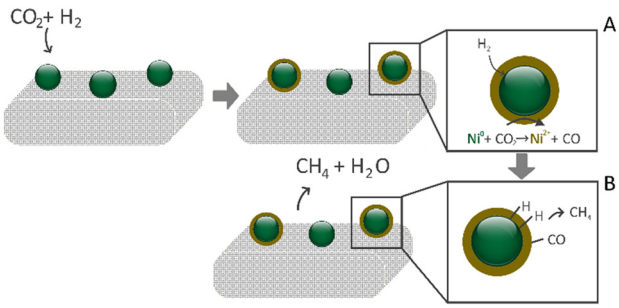

Fig. 5 Schematic representation of the hypothesized mechanism of the Ni@NiO nanostructure formation during CO_2 methanation over the high-performance Ni/ACR catalyst. Box A – the Ni oxide shell structure is formed *in situ* (Ni^0 + CO_2 → NiO + CO), allowing for the penetration of H_2 to the active metallic Ni^0 core; box B – Ni oxide shell acts as an enhancer of the CO_2 adsorption/activation while the Ni^0 in the core is responsible for H_2 dissociation, leading to both reactants in close proximity, facilitating the CH_4 formation.

of CO_2 methanation, and it is expected to be an integral part of the reaction process. Fig. 5 presents a summary of the findings of this work. We believe that the Ni oxide shell structure, *in situ* formed during methanation, exhibits a permeable nature, allowing for the penetration of the reaction CO_2 and H_2 gases to the active metallic Ni^0 core, otherwise dynamic changes under reaction conditions would not continue to be observed in the nanoparticles demonstrating a shell. We hypothesize that the Ni oxide shell acts as an enhancer of the CO_2 adsorption/activation, while the Ni^0 in the core is responsible for H_2 dissociation, which leads to both reactants being in close proximity, facilitating the CH_4 formation.[35,36] Notably, we observed *in situ* that the main deactivation mechanism was related to a particle size.

3 Conclusions

In summary, we have presented an *in situ* TEM investigation of our previously reported high-performance nickel nanoparticle catalyst supported on reduced activated carbon.[3] The unprecedented *in situ* formation of a NiO shell around the metallic Ni^0 core was directly imaged and studied under CO_2 methanation conditions. An important proposed feature of real Ni@NiO core@shell catalyst nanoparticles is coupling of the enhanced CO_2 adsorption/activation over the NiO shell with H_2 dissociation over the Ni^0 core, bringing the reactants and intermediates together to accomplish CO_2 hydrogenation into CH_4. This fundamental understanding of CO_2 methanation over the Ni catalyst provides a framework for the judicious design and realization of new high-performance and stable core@shell catalysts for this reaction, in particular, and other interesting CO_2 hydrogenation reactions, in general.

Data availability

Data for this article are available in the ESI.†

Author contributions

Katherine E. MacArthur: conceptualization, data curation, formal analysis, investigation, methodology, and writing – original draft; Liliana P. L. Gonçalves: conceptualization, formal analysis, investigation, methodology, and writing – original draft; Juliana P. S. Sousa: supervision and writing – review & editing; O. Salomé G. P. Soares: conceptualization, supervision, and writing – review & editing; Hans Kungl: writing – review & editing; Eva Jodat: writing – review & editing; André Karl: writing – review & editing; Marc Heggen: writing – review & editing; Rafal E. Dunin-Borkowski: funding acquisition, project administration, and writing – review & editing; Shibabrata Basak: conceptualization, data curation, investigation, methodology, writing – review & editing, and supervision; Rüdiger-A. Eichel: writing – review & editing; Yury V. Kolen'ko: conceptualization, funding acquisition, project administration, resources, supervision, and writing – review & editing; M. Fernando R. Pereira: conceptualization, funding acquisition, project administration, resources, supervision, and writing – review & editing.

Conflicts of interest

There are no conflicts to declare.

Acknowledgements

The authors gratefully acknowledge the support of the German Research Foundation (DFG) for supporting this work under grant number HE 7192/1-2. S. B. acknowledges support for the project 'Electroscopy' (Grant No. 892916) from the Marie Skłodowska-Curie action. L. P. L. G. thanks the Portuguese Foundation for Science and Technology (FCT) for the PhD grant (SFRH/BD/128986/2017). This work was partially supported by national funds through Fundação para a Ciência e a Tecnologia, I.P./MCTES: LSRE-LCM, UID/50020; ALiCE, LA/P/0045/2020 (DOI: **https://doi.org/10.54499/LA/P/0045/2020**). O. S. G. P. S. acknowledges FCT funding under the Scientific Employment Stimulus – Institutional Call (CEECINST/00049/2018).

References

1 M. Bailera, P. Lisbona, L. M. Romeo and S. Espatolero, Power to gas projects review: Lab, pilot and demo plants for storing renewable energy and CO_2, *Renewable Sustainable Energy Rev.*, 2017, **69**, 292–312.

2 J. Ashok, S. Pati, P. Hongmanorom, Z. Tianxi, C. Junmei and S. Kawi, A review of recent catalyst advances in CO_2 methanation processes, *Catal. Today*, 2020, **356**, 471–489.

3 L. P. L. Gonçalves, J. P. S. Sousa, O. S. G. P. Soares, O. Bondarchuk, O. I. Lebedev, Y. V. Kolen'ko and M. F. R. Pereira, The role of surface properties in CO_2 methanation over carbon-supported Ni catalysts and their promotion by Fe, *Catal. Sci. Technol.*, 2020, **10**, 7217.

4 B. Miao, S. S. K. Ma, X. Wang, H. Su and S. H. Chan, Catalysis mechanisms of CO_2 and CO methanation, *Catal. Sci. Technol.*, 2016, **6**, 4048–4058.

5 F. Goodarzi, L. Kang, F. R. Wang, F. Joensen, S. Kegnæs and J. Mielby, Methanation of carbon dioxide over zeolite-encapsulated nickel nanoparticles, *ChemCatChem*, 2018, **10**, 1566–1570.

6 Z. Zhang, Y. Tian, L. Zhang, S. Hu and J. Xiang, Impacts of nickel loading on properties, catalytic behaviors of Ni/γ–Al_2O_3 catalysts and the reaction intermediates formed in methanation of CO_2, *Int. J. Hydrogen Energy*, 2019, **44**, 9291–9306.

7 Y. Ma, J. Liu, M. Chu, J. Yue, Y. Cui and G. Xu, Cooperation between active metal and basic support in Ni-based catalyst for low-temperature CO_2 methanation, *Catal. Lett.*, 2020, **150**, 1418–1426.

8 X. Wen, L. Xu, M. Chen, Y. Shi, C. Lv, Y. Cui, X. Wu, G. Cheng, C. E. Wu, Z. Miao, F. Wang and X. Hu, Exploring the influence of nickel precursors on constructing efficient Ni-

based CO_2 methanation catalysts assisted with in-situ technologies, *Appl. Catal., B*, 2021, **297**, 120486.

9 A. Westermann, B. Azambre, M. C. Bacariza, I. Graça, M. F. Ribeiro, J. M. Lopes and C. Henriques, Insight into CO_2 methanation mechanism over NiUSY zeolites: An operando IR study, *Appl. Catal., B*, 2015, **174–175**, 120–125.

10 W. Zhen, B. Li, G. Lu and J. Ma, Enhancing catalytic activity and stability for CO_2 methanation on Ni@MOF-5 via control of active species dispersion, *Chem. Commun.*, 2015, **51**, 1728–1731.

11 L. P. L. Gonçalves, A. Serov, G. McCool, M. Dicome, J. P. S. Sousa, O. S. G. P. Soares, O. Bondarchuk, D. Y. Petrovykh, O. I. Lebedev, M. F. R. Pereira and Y. V. Kolen'ko, New opportunity for carbon-supported Ni-based electrocatalysts: Gas-phase CO_2 methanation, *ChemCatChem*, 2021, **13**, 4770–4779.

12 N. N. Ha, N. T. Ha, L. V. Khu and L. M. Cam, Theoretical study of carbon dioxide activation by metals (Co, Cu, Ni) supported on activated carbon, *J. Mol. Model.*, 2015, **21**, 322.

13 W. Wang, C. Duong-Viet, H. Ba, W. Baaziz, G. Tuci, S. Caporali, L. Nguyen-Dinh, O. Ersen, G. Giambastiani and C. Pham-Huu, Nickel nanoparticles decorated nitrogen-doped carbon nanotubes (Ni/N-CNT); A robust catalyst for the efficient and selective CO_2 methanation, *ACS Appl. Energy Mater.*, 2019, **2**, 1111–1120.

14 J. Gödde, M. Merko, W. Xia and M. Muhler, Nickel nanoparticles supported on nitrogen–doped carbon nanotubes are a highly active, selective and stable CO_2 methanation catalyst, *J. Energy Chem.*, 2021, **54**, 323–331.

15 P. Kangvansura, L. M. Chew, W. Saengsui, P. Santawaja, Y. Poo-arporn, M. Muhler, H. Schulz and A. Worayingyong, Product distribution of CO_2 hydrogenation by K- and Mn-promoted Fe catalysts supported on N-functionalized carbon nanotubes, *Catal. Today*, 2016, **275**, 59–65.

16 W. Wang, W. Chu, N. Wang, W. Yang and C. Jiang, Mesoporous nickel catalyst supported on multi-walled carbon nanotubes for carbon dioxide methanation, *Int. J. Hydrogen Energy*, 2015, **41**, 967–975.

17 J. Gao, Q. Jiang, Y. Liu, W. Liu, W. Chu and D. S. Su, Probing the enhanced catalytic activity of carbon nanotube supported Ni-LaOx hybrids for the CO_2 reduction reaction, *Nanoscale*, 2018, **10**, 14207–14219.

18 M. Romero-Sáez, A. B. Dongil, N. Benito, R. Espinoza-González, N. Escalona and F. Gracia, CO_2 methanation over nickel-ZrO_2 catalyst supported on carbon nanotubes: A comparison between two impregnation strategies, *Appl. Catal., B*, 2018, **237**, 817–825.

19 A. I. Tsiotsias, N. D. Charisiou, I. V. Yentekakis and M. A. Goula, Bimetallic Ni-based catalysts for CO_2 methanation: A review, *Nanomaterials*, 2021, **11**, 28.

20 Y. H. Lee, J. Y. Ahn, D. D. Nguyen, S. W. Chang, S. S. Kim and S. M. Lee, Role of oxide support in Ni based catalysts for CO_2 methanation, *RSC Adv.*, 2021, **11**, 17648–17657.

21 P. A. U. Aldana, F. Ocampo, K. Kobl, B. Louis, F. Thibault-Starzyk, M. Daturi, P. Bazin, S. Thomas and A. C. Roger, Catalytic CO_2 valorization into CH_4 on Ni-based ceria-zirconia. Reaction mechanism by operando IR spectroscopy, *Catal. Today*, 2013, **215**, 201–207.

22 L. P. L. Gonçalves, J. Mielby, O. S. G. P. Soares, J. P. S. Sousa, D. Y. Petrovykh, O. I. Lebedev, M. F. R. Pereira, S. Kegnæs and Y. V. Kolen'ko, In situ investigation of the CO_2 methanation on carbon/ceria-supported Ni catalysts using modulation-excitation DRIFTS, *Appl. Catal., B*, 2022, **312**, 121376.

23 Z. Hao, J. Shen, S. Lin, X. Han, X. Chang, J. Liu, M. Li and X. Ma, Decoupling the effect of Ni particle size and surface oxygen deficiencies in CO_2 methanation over ceria supported Ni, *Appl. Catal., B*, 2021, **286**, 119922.

24 H. L. Huynh, J. Zhu, G. Zhang, Y. Shen, W. M. Tucho, Y. Ding and Z. Yu, Promoting effect of Fe on supported Ni catalysts in CO_2 methanation by in situ DRIFTS and DFT study, *J. Catal.*, 2020, **392**, 266–277.

25 A. Cárdenas-Arenas, A. Quindimil, A. Davó-Quiñonero, E. Bailón-García, D. Lozano-Castelló, U. De-La-Torre, B. Pereda-Ayo, J. A. González-Marcos, J. R. González-Velasco and A. Bueno-López, Isotopic and in situ DRIFTS study of the CO_2 methanation mechanism using Ni/CeO_2 and Ni/Al_2O_3 catalysts, *Appl. Catal., B*, 2020, **265**, 118538.

26 G. Giorgianni, C. Mebrahtu, M. E. Schuster, A. I. Large, G. Held, P. Ferrer, F. Venturini, D. Grinter, R. Palkovits, S. Perathoner, G. Centi, S. Abate and R. Arrigo, Elucidating the mechanism of the CO_2 methanation reaction over Ni–Fe hydrotalcite-derived catalysts via surface-sensitive in situ XPS and NEXAFS, *Phys. Chem. Chem. Phys.*, 2020, **22**, 18788–18797.

27 S. K. Beaumont, S. Alayoglu, C. Specht, W. D. Michalak, V. V. Pushkarev, J. Guo, N. Kruse and G. A. Somorjai, Combining in situ NEXAFS spectroscopy and CO_2 methanation kinetics to study Pt and Co nanoparticle catalysts reveals key insights into the role of platinum in promoted cobalt catalysis, *J. Am. Chem. Soc.*, 2014, **136**, 9898–9901.

28 P. Strucks, L. Failing and S. Kaluza, A short review on Ni-catalyzed methanation of CO_2: Reaction mechanism, catalyst deactivation, dynamic operation, *Chem. Ing. Tech.*, 2021, **93**, 1526–1536.

29 C. Heine, B. A. J. Lechner, H. Bluhm and M. Salmeron, Recycling of CO_2: Probing the chemical state of the Ni(111) surface during the methanation reaction with ambient-pressure X-ray photoelectron spectroscopy, *J. Am. Chem. Soc.*, 2016, **138**, 13246–13252.

30 B. Mutz, H. W. P. Carvalho, S. Mangold, W. Kleist and J. D. Grunwaldt, Methanation of CO_2: Structural response of a Ni-based catalyst under fluctuating reaction conditions unraveled by operando spectroscopy, *J. Catal.*, 2015, **327**, 48–53.

31 G. Zhou, H. Liu, K. Cui, A. Jia, G. Hu, Z. Jiao, Y. Liu and X. Zhang, Role of surface Ni and Ce species of Ni/CeO_2 catalyst in CO_2 methanation, *Appl. Surf. Sci.*, 2016, **383**, 248–252.

32 Y. Du, C. Qin, Y. Xu, D. Xu, J. Bai, M. Ding, C. Qin, Y. Xu, D. Xu, J. Bai and M. Ding, Ni nanoparticles dispersed on oxygen vacancies-rich CeO_2 nanoplates for enhanced low-temperature CO_2 methanation performance, *Chem. Eng. J.*, 2021, **417**, 129402.

33 C. Vogt, E. Groeneveld, G. Kamsma, M. Nachtegaal, L. Lu, C. J. Kiely, P. H. Berben, F. Meirer and B. M. Weckhuysen, Unravelling structure sensitivity in CO_2 hydrogenation over nickel, *Nat. Catal.*, 2018, **1**, 127–134.